Electronic Supplementary Material (ESI) for Chemical Communications.

Supporting information

Boron-Hyperdoped Silicon for the Selective Oxidative Dehydrogenation of Propane to Propylene

Junjie Chen[a], Parham Rohani[a], Stavros G. Karakalos[b], Michael J. Lance[c], Todd J. Toops[d], Mark T. Swihart[a], Eleni A. Kyriakidou[a,*]

[a] *Department of Chemical and Biological Engineering, University at Buffalo, The State University of New York, Buffalo, NY 14260, USA*

[b] *Department of Chemical Engineering, University of South Carolina, Columbia, SC, 29208, USA*

[c] *Materials Science and Technology Division, Oak Ridge National Laboratory, Oak Ridge, TN, USA*

[d] *Energy and Transportation Sciences Division, Oak Ridge National Laboratory, Oak Ridge, TN, USA*

List of contents

1. Catalyst synthesis

The synthesis of pure silicon and boron-hyperdoped silicon (15, 25, and 42 at.% or 6.4, 11.4, and 21.7 wt.%, respectively) was described in detail previously.[12] For the production of boron-hyperdoped silicon samples with different boron concentrations, specific flows of silane and diborane in hydrogen (200 sccm) were introduced into a reaction chamber where it was exposed to a 100 W continuous CO_2 laser. The wavelength of the infrared laser beam was 10.6 μm. Silane can absorb the laser energy and transfer it to the diborane molecules by intermolecular collisions. This produces rapid heating, decomposing the silane and diborane and initiating particle formation. The total reactant gas flow was ~2730 sccm and the reactor pressure was ~8 psia.

21.7 wt.% B/SiO_2 (same B weight concentration as the 42 at.% boron-hyperdoped silicon sample) was synthesized by wet impregnation of boric acid (Sigma-Aldrich, ACS reagent, ≥99.5%) in silica gel (Sigma-Aldrich, BET surface area ~500 m^2/g). The catalyst was dried at 110 ^oC overnight and calcined at 500 ^oC in air for 2 h with a temperature ramp of 10 ^oC/min.

Porous BN with surface area (43.8 m^2/g) higher than that of commercial h-BN (9.1 m^2/g) was synthesized as reported previously.[13] Briefly, 9 g of urea (Sigma-Aldrich, ACS reagent, 99.0-100.5%) and 1.85 g of boric acid were dissolved in 450 mL D.I. water, followed by a complete water evaporation at 65 ^oC while keep stirring. The resulting powder was calcined at 1050 ^oC for 3.5 h (10 ^oC/min) under 50 sccm N_2.

2. Catalyst characterization

TEM images of pure silicon and boron-hyperdoped silicon were collected with a JEOL 2010 microscope. STEM images and EDS elemental maps were collected with a FEI Talos F200X STEM. The BET surface areas and BJH pore volumes were measured by N_2 physisorption (Tri-Star II, Micromeritics). Before the BET and BJH measurements all samples were degassed at 150 ^oC for 2 h. FTIR spectra of quartz sand, pure silicon and boron-hyperdoped silicon samples were collected by a Bruker Vertex 70 FTIR spectrometer. X-ray photoelectron spectroscopy (XPS) was collected with a Kratos AXIS Ultra DLD XPS (Kratos Analytical). The XPS system is equipped with a monochromatic Al Kα source and operated at 15 keV and 150 W. High-resolution core level spectra were measured with a pass energy of 40 eV.

3. Catalyst evaluation

The ODHP performance of boron-hyperdoped silicon samples was evaluated in a packed bed reactor similar to the ones reported previously.[14-16] In each case, 25 mg sample diluted with

100 mg quartz sand was loaded in a U-shaped quartz reactor. The reactor feed consisted of C_3H_8:O_2:Ar at 1:1.5:3.5 ratios with a total flow of 36 sccm (WHSV=28.2 $g_{C_3H_8}$ g_{cat}^{-1} h^{-1}) under ambient pressure (1 atm). Pure silicon, 15, 25, and 42 at.% boron-hyperdoped silicon samples were initially pretreated at 460 °C for 5 h under reaction conditions (C_3H_8:O_2:Ar = 1:1.5:3.5, total flow = 36 sccm). Commercial h-BN (Alfa aesar, surface area = 9.1 m^2/g), porous BN, and 21.7 wt.% B/SiO_2 were activated at 535 °C under reaction conditions (C_3H_8:O_2:Ar = 1:1.5:3.5, total flow = 36 sccm) as reported previously.[11] After the completion of the pretreatment the catalysts were step-wisely cooled down to 450-400 °C (pure silicon and boron-hyperdoped silicon samples) and 500-450 °C (commercial h-BN, porous BN, and 21.7 wt.% B/SiO_2). An online MKS FTIR gas analyzer (MultiGas 2030) was used to continuously monitor the concentrations of reactant (C_3H_8) and products (C_3H_6, C_2H_4, C_2H_6, C_2H_2, CH_4, CH_3CHO, HCHO, CH_3OH, HCOOH, CO_2, CO, H_2O). Product selectivities and C_3H_8 conversions were obtained from30 min under steady state.

C_3H_8 conversion was calculated as shown in Eq. (1).

$$\textit{C}_3\textit{H}_8\textit{ conversion:}\quad X = \frac{(C_{C_3H_8,in} - C_{C_3H_8,out})}{C_{C_3H_8,in}} \times 100\% \tag{1}$$

The C_3H_6 selectivity was calculated as shown in Eq. (2).

C_3H_6 selectivity:

$$S_{C_3H_6} = 3 \times C_{C_3H_6,out} \times \begin{pmatrix} 3 \times C_{C_3H_6,out} + 2 \times C_{C_2H_4,out} + \\ 2 \times C_{C_2H_6,out} + 2 \times C_{C_2H_2,out} + \\ C_{CH_4,out} + 2 \times C_{CH_3CHO,out} + \\ C_{HCHO,out} + C_{CH_3OH,out} + \\ C_{HCOOH,out} + C_{CO_2,out} + C_{CO,out} \end{pmatrix}^{-1} \times 100\% \tag{2}$$

The apparent activation energies were calculated using the Arrhenius equation.

Table S1. BET surface area and BJH pore volume of pure silicon, and 15, 25 and 42 at.% boron-hyperdoped silicon samples.

Sample	Surface area (BET) (m^2/g)	Pore volume (BJH) (cm^3/g)
pure silicon	101.4	0.356
15 at.% boron-hyperdoped silicon	88.9	0.405
25 at.% boron-hyperdoped silicon	96.6	0.398
42 at.% boron-hyperdoped silicon	94.6	0.370

Table S2. Summary of conversion (X), selectivity (S) and productivity of ODHP catalysts reported in literature.

Catalyst	T (℃)	WHSV* ($g_{C_3H_8} g_{cat}^{-1} h^{-1}$)	$X_{C_3H_8}$ (%)	$S_{C_3H_6}$ (%)	$S_{C_2H_4}$ (%)	S_{CO} (%)	S_{CO_2} (%)	C_3H_6 productivity ($g_{C_3H_6} g_{cat}^{-1} h^{-1}$)	Olefin productivity ($g_{olefin} g_{cat}^{-1} h^{-1}$)	Ref.
pure silicon	450	28.2	0.12	40.3	3.6	5.8	43.6	0.01	0.01	This work
15 at.% boron-hyperdoped silicon	450	28.2	5.2	67.1	6.2	7.6	4.6	0.94	1.03	This work
25 at.% boron-hyperdoped silicon	450	28.2	10.6	64.1	7.2	9.7	2.5	1.83	1.97	This work
42 at.% boron-hyperdoped silicon	450	28.2	5.0	75.6	5.6	5.73	0.5	1.02	1.07	This work
Commercial h-BN	450	28.2	0.7	83.6	2.8	4.0	~0	0.16	0.16	This work
porous BN	450	28.2	1.0	79.4	2.7	4.0	7.0	0.21	0.22	This work
21.7 wt.% B/SiO_2	450	28.2	0.5	78.1	2.3	3.8	8.9	0.11	0.11	This work
BOS-10	500	9.4	31.5	64.0	19.1	14.8	2.1	2.06	2.47	[1]
Silicon boride	535	9.4	19.2	82.2	12.2	n.a.	n.a.	1.42	1.56	[2]
B_4C	500	10.7	7.0	84.2	9.3	3.4	0.7	0.6	0.64	[3]
Ti_2B	500	10.6	5.8	85.4	9.1	2.6	0.4	0.5	0.54	[3]
NiB	500	8.0	6.1	85.4	9.3	2.2	0.3	0.4	0.41	[3]
BNOH	530	37.6	20.6	80.2	10.7	7.9	0.5	5.93	6.46	[11]
V–MgO	500	11.8	24	57.5	n.a.	27.2	15.3	1.55	1.45	[4]
V_2O_5/SBA-15	550	14.1	25.3	65.4	6.2	n.a.	25.2	2.23	2.47	[5]

Continued with **Table S2**

Catalyst	**T (℃)**	**WHSV*** ($g_{C_3H_8} g_{cat}^{-1} h^{-1}$)	$X_{C_3H_8}$ **(%)**	$S_{C_3H_6}$ **(%)**	$S_{C_2H_4}$ **(%)**	S_{CO} **(%)**	S_{CO_2} **(%)**	C_3H_6 **productivity** ($g_{c_3H_6} g_{cat}^{-1} h^{-1}$)	**Olefin productivity** ($g_{olefin} g_{cat}^{-1} h^{-1}$)	**Ref.**
VOx/MCM-41	550	8.8	16.5	45.5	n.a.	33.8	14.9	0.63	0.59	[6]
F–V_2O_5/SiO_2	540	3	14.8	64.2	n.a.	n.a.	n.a.	0.27	0.27	[7]
$ZrV_{0.15}O_x$	540	8.8	24.4	39.9	n.a.	n.a.	45.6	0.82	0.9	[8]
SrVMoOx/Al_2O_3	500	5.3	22	67.8	n.a.	n.a.	28	0.75	0.75	[9]
Cr_2O_3/SBA-15	550	4.9	20.5	33.2	25.9	16.7	22.2	0.32	0.52	[10]

*WHSV: Weight Hourly Space Velocity.

Table S3. Apparent activation energies of the ODHP reaction over 15, 25, 42 at.% boron-hyperdoped silicon, commercial h-BN, porous BN, and 21.7 wt.% B/SiO_2 samples.

Sample	Ea (kJ/mol)
15 at.% boron-hyperdoped silicon	148.6
25 at.% boron-hyperdoped silicon	160.5
42 at.% boron-hyperdoped silicon	159.0
commercial h-BN	180.0
porous BN	188.3
21.7 wt.% B/SiO_2	186.2

Table S4. Surface composition of pure silicon, 15, 25, and 42 at.% boron-hyperdoped silicon samples determined by XPS.

Sample	Si (%)	B (%)	C (%)	O (%)	B/(Si + B)
pure silicon	66.2	-	4.7	29.1	-
15 at.% boron-hyperdoped silicon	37.7	18.9	6.0	37.4	33.3
25 at.% boron-hyperdoped silicon	31.4	23.5	5.9	39.2	42.8
42 at.% boron-hyperdoped silicon	30.0	27.5	5.0	37.6	47.8

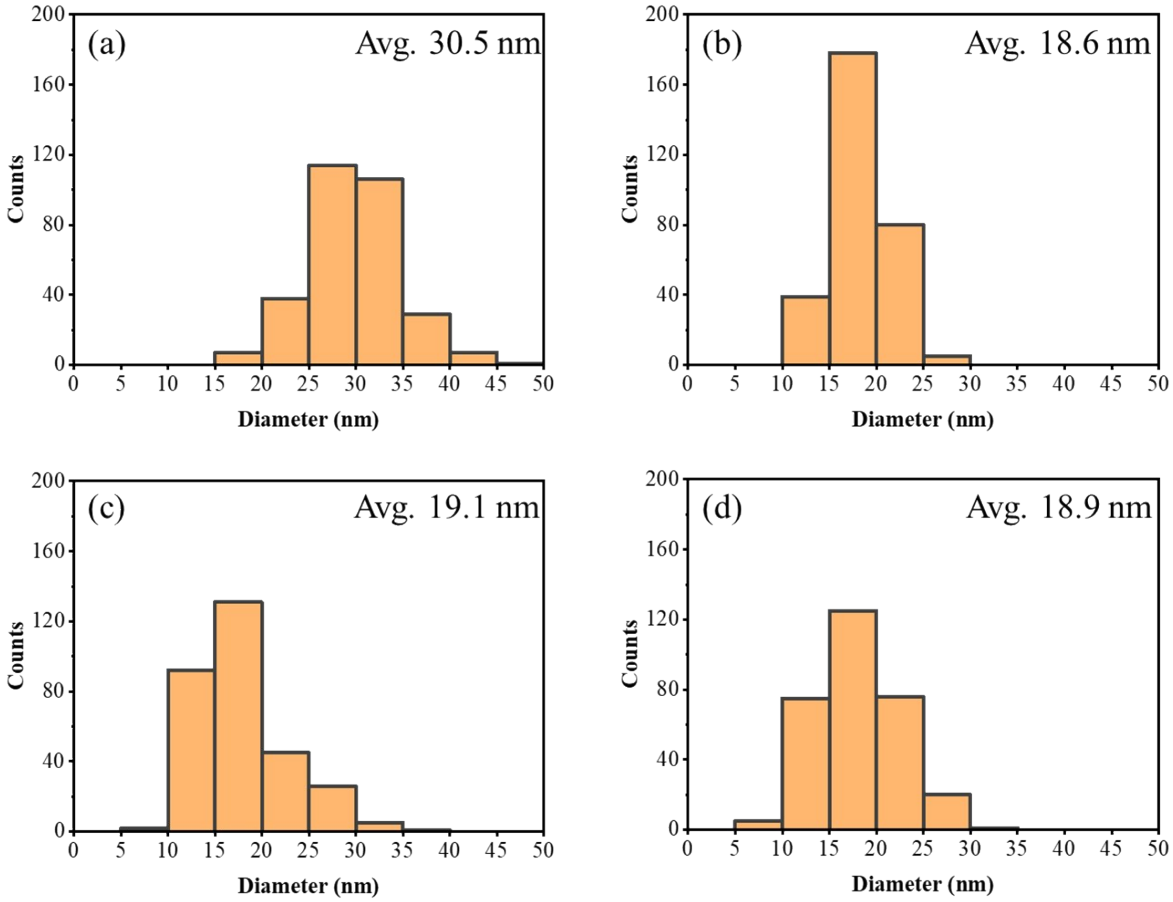

Fig. S1. Particle size distributions based on TEM images of (a) pure silicon and (b) 15 at.%, (c) 25 at.% and (d) 42 at.% boron-hyperdoped silicon catalysts.

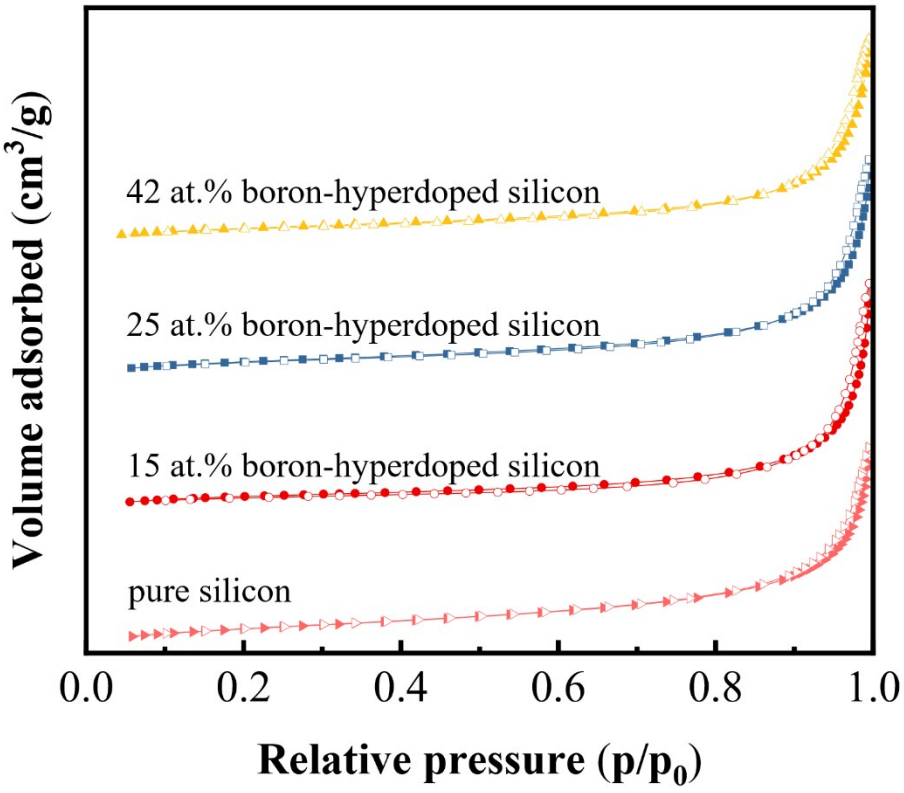

Fig. S2. N_2 adsorption (solid) and desorption (open) isotherms of pure silicon, 15, 25, and 42 at.% boron-hyperdoped silicon catalysts.

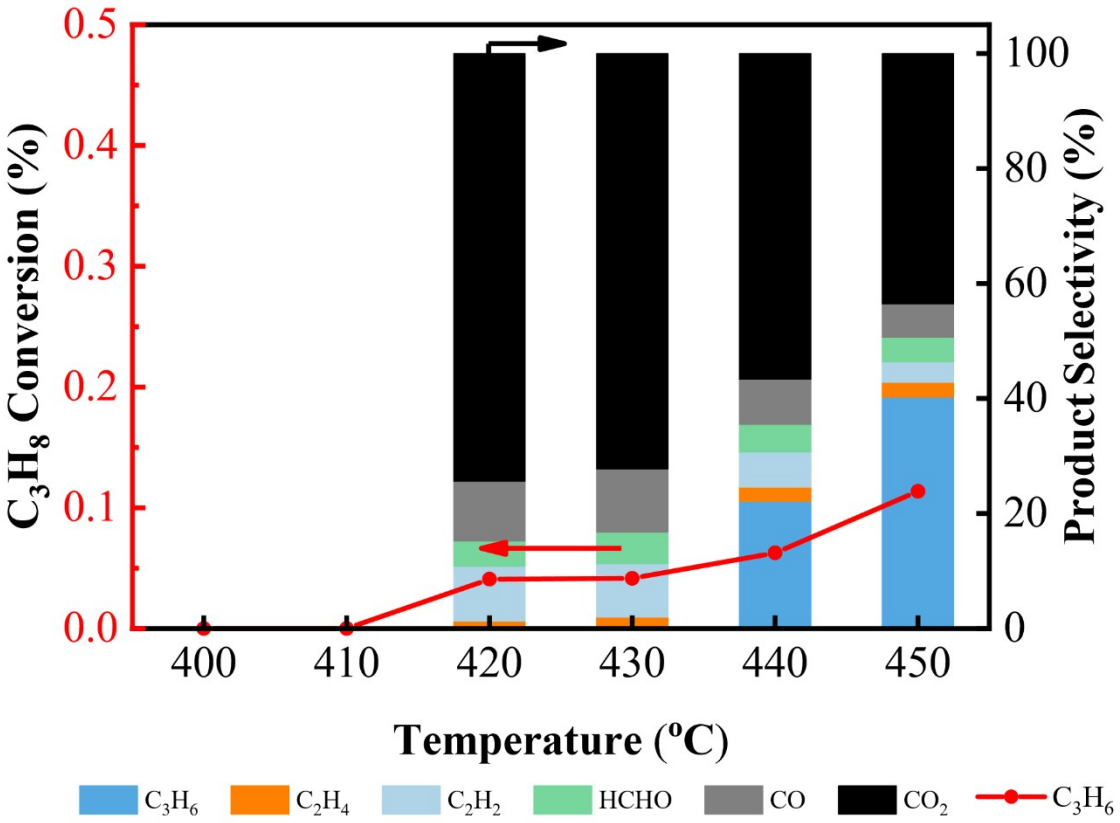

Fig. S3. C_3H_8 conversion and product selectivity as a function of temperature over pure silicon (0% C_3H_8 conversion was observed at 400 and 410 °C).

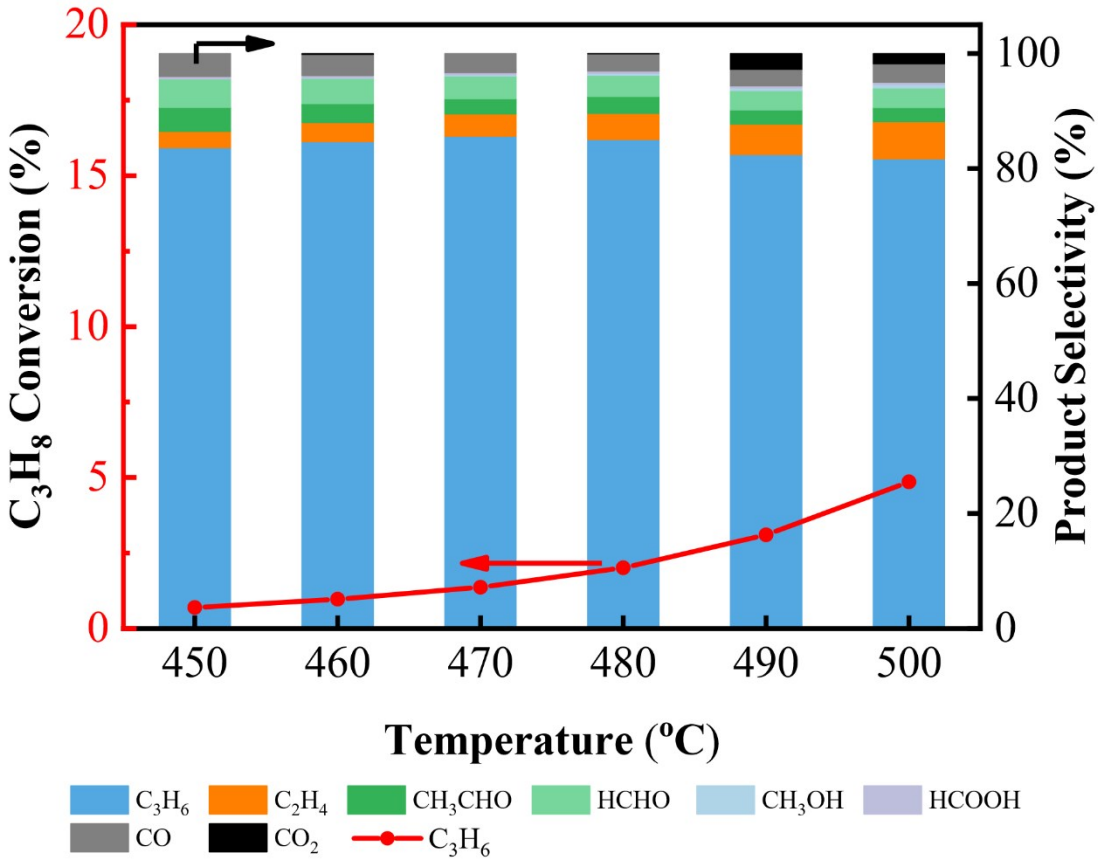

Fig. S4. C_3H_8 conversion and product selectivity as a function of temperature over activated commercial h-BN.

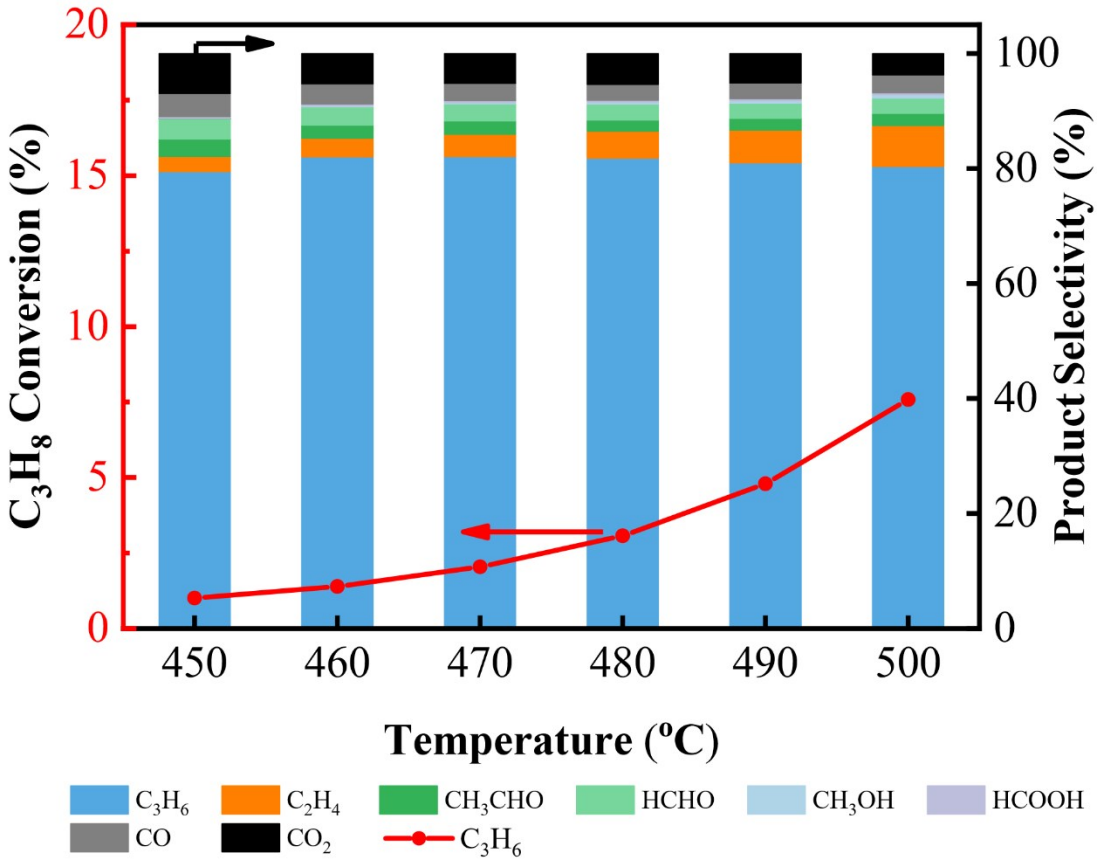

Fig. S5. C_3H_8 conversion and product selectivity as a function of temperature over activated porous BN.

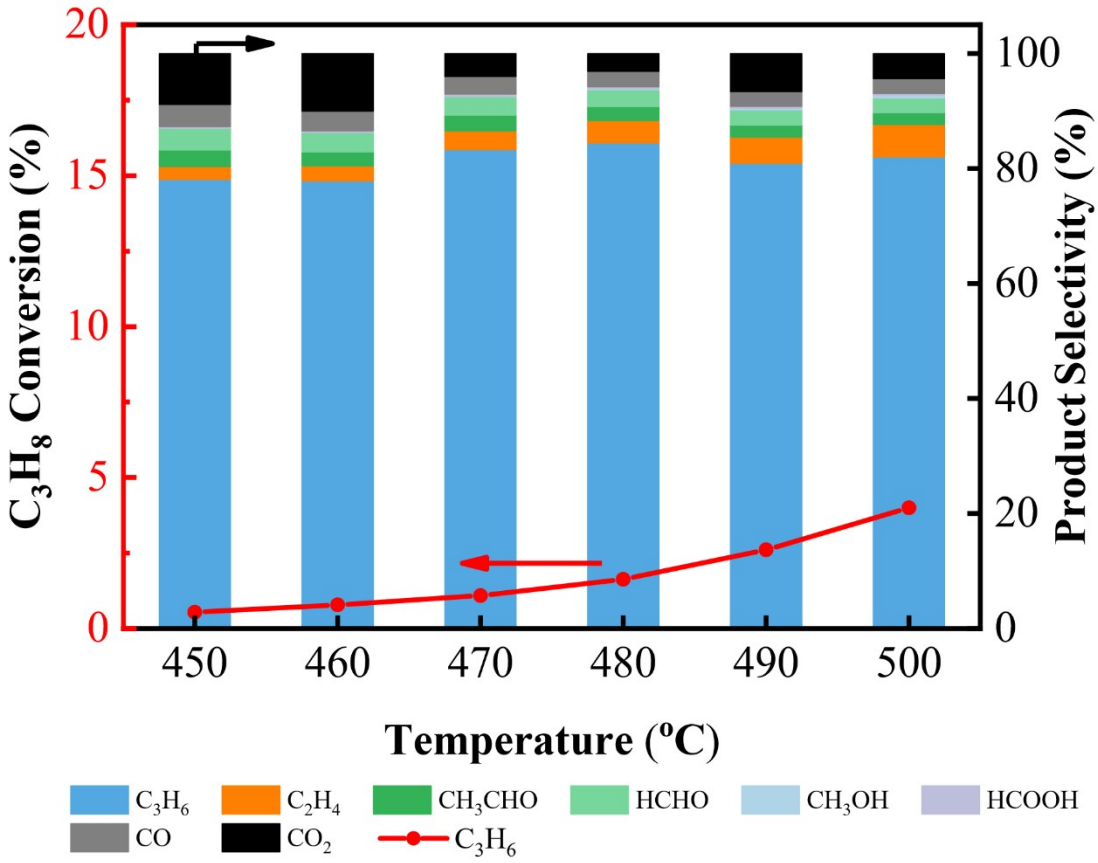

Fig. S6. C_3H_8 conversion and product selectivity as a function of temperature over activated 21.7 wt.% B/SiO_2.

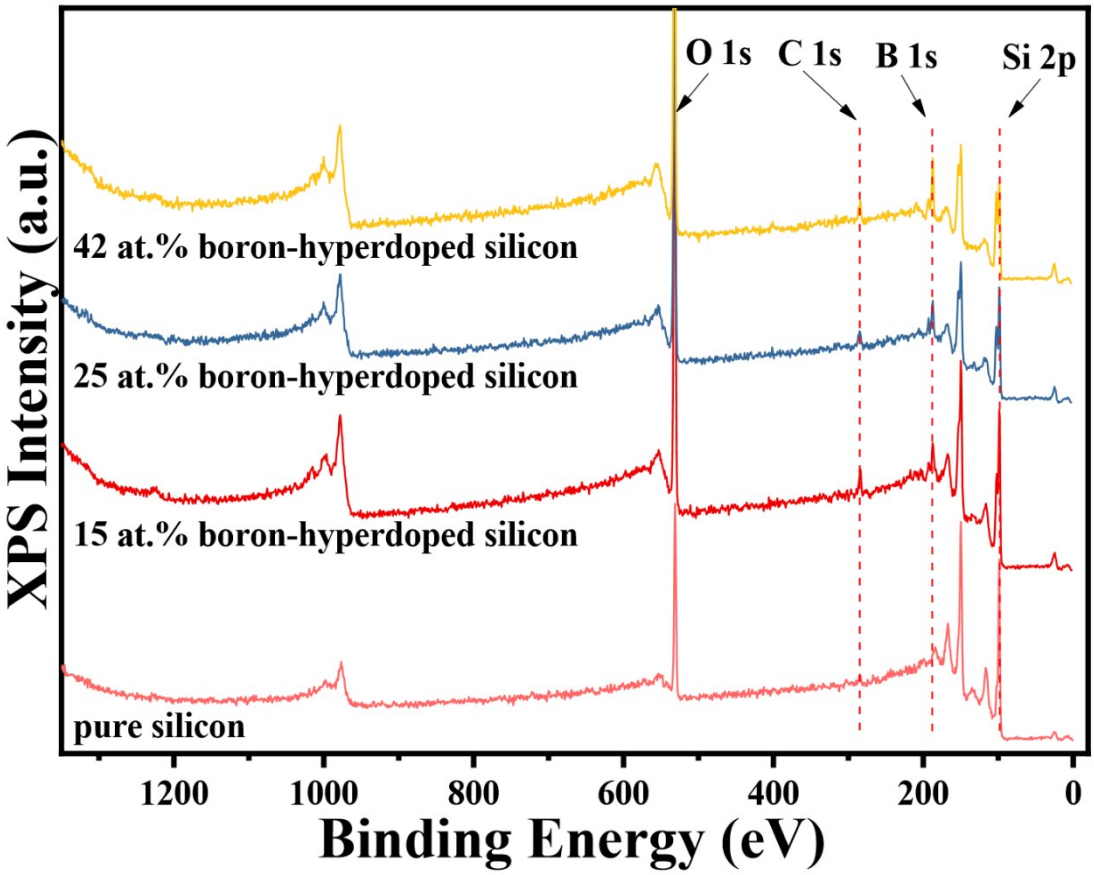

Fig. S7. XPS survey scans of pure silicon, 15, 25, and 42 at.% boron-hyperdoped silicon samples.

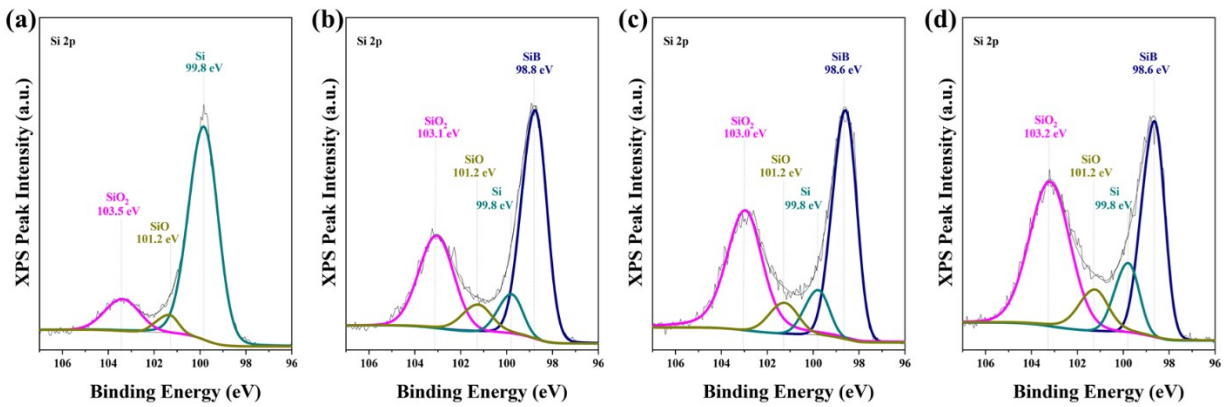

Fig. S8. Si 2p XPS spectra of (a) pure silicon, (b) 15, (c) 25, and (d) 42 at.% boron-hyperdoped silicon samples.

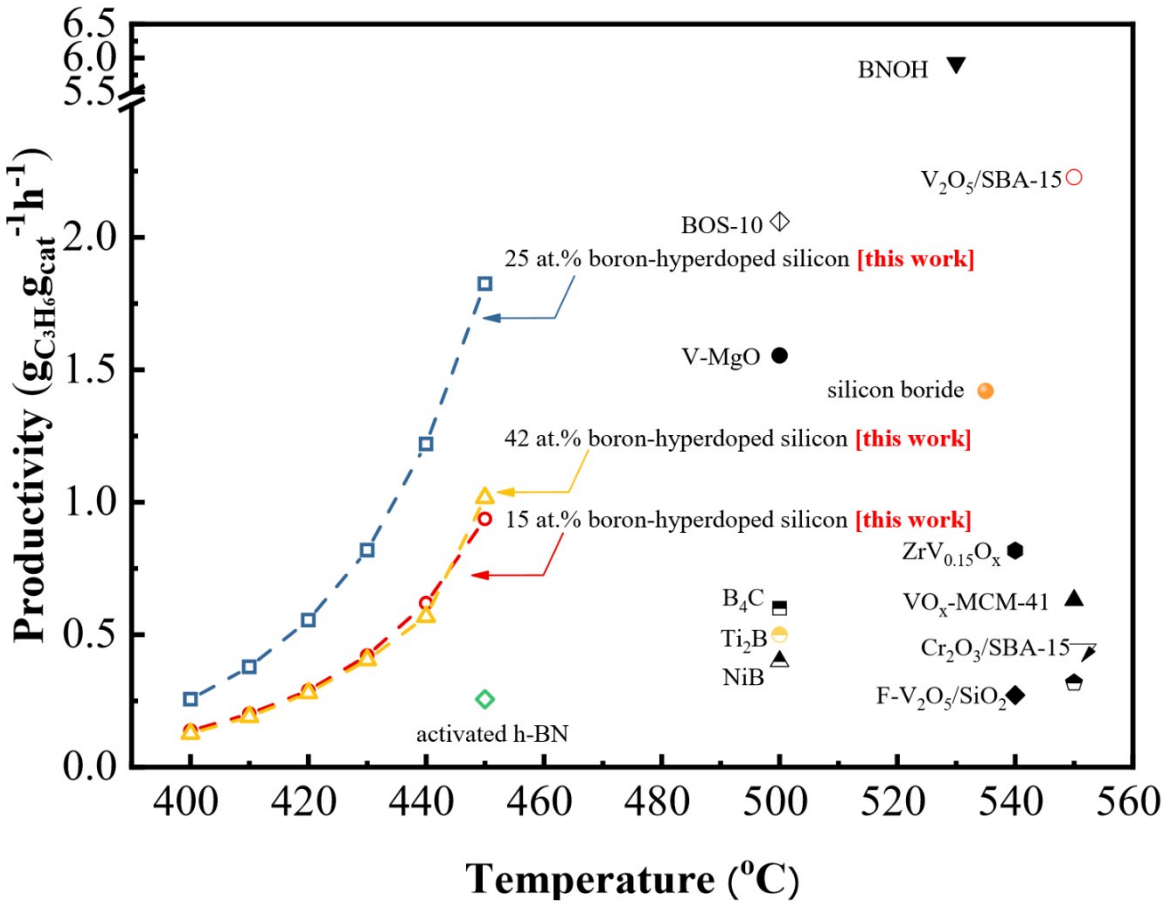

Fig. S9. Comparison of the C_3H_6 productivity of boron-hyperdoped silicon with other reported catalysts[1-11] as a function of reaction temperature.

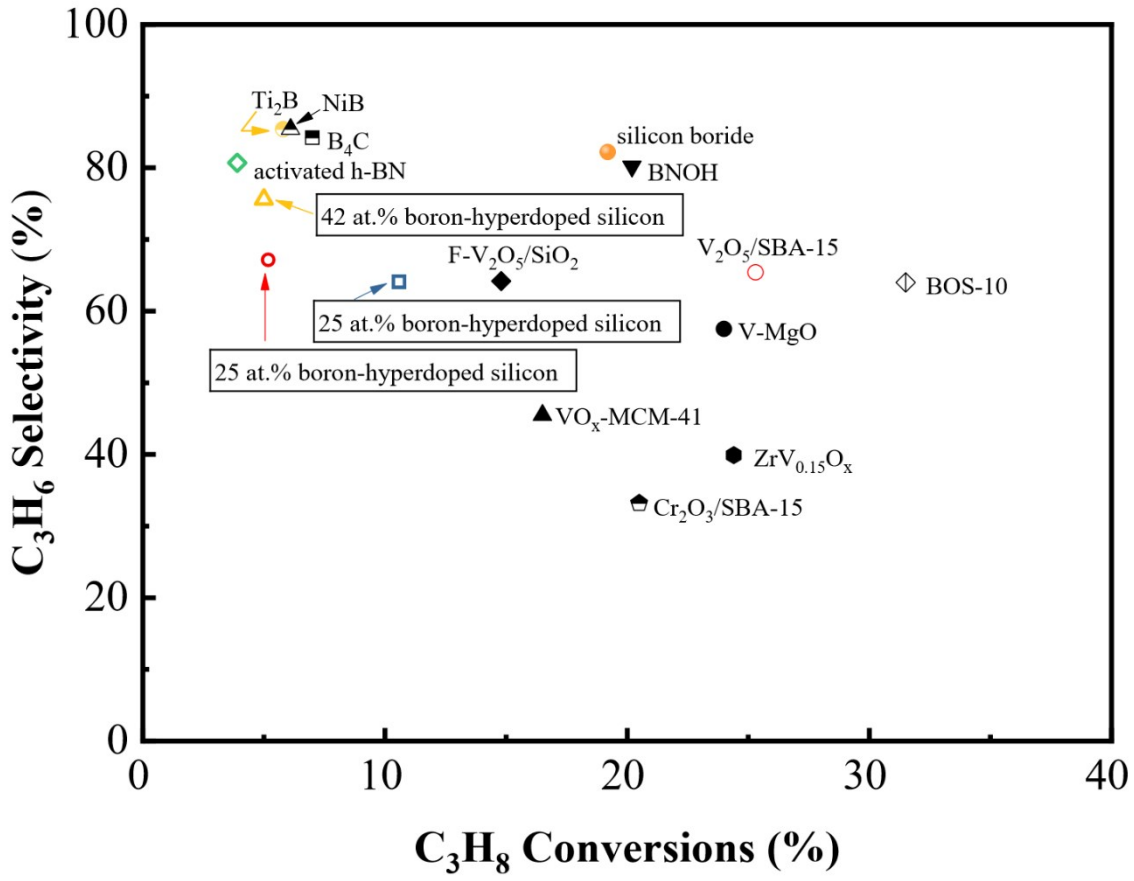

Fig. S10. Comparison of the C_3H_6 selectivity vs. C_3H_8 conversion of boron-hyperdoped silicon with other reported catalysts[1-11]. Catalysts marked with a box are the ones reported in this work.

References:

1. W.-D. Lu, D. Wang, Z. Zhao, W. Song, W.-C. Li and A.-H. Lu, *ACS Catal.*, 2019, **9**, 8263-8270.
2. B. Yan, W.-C. Li and A.-H. Lu, *J. Catal.*, 2019, **369**, 296-301.
3. J. T. Grant, W. P. McDermott, J. M. Venegas, S. P. Burt, J. Micka, S. P. Phivilay, C. A. Carerro and I. Hermans, *ChemCatChem*, 2017, **9**, 3623-3626.
4. E. Kondratenko, O. Buyevskaya and M. Baerns, *Top. Catal.*, 2001, **15**, 175-180.
5. Y.-M. Liu, W.-L. Feng, T.-C. Li, H.-Y. He, W.-L. Dai, W. Huang, Y. Cao and K.-N. Fan, *J. Catal.*, 2006, **239**, 125-136.
6. B. Solsona, T. Blasco, J. L. Nieto, M. Pena, F. Rey and A. Vidal-Moya, *J. Catal.*, 2001, **203**, 443-452.
7. Y. Liu, C. Jiang, W. Chu, W. Sun and Z. Xie, *React. Kinet. Mech. Catal.*, 2010, **101**, 141-151.
8. S. Chen, F. Ma, A. Xu, L. Wang, F. Chen and W. Lu, *Appl. Surf.Sci.*, 2014, **289**, 316-325.
9. M. D. Putra, S. M. Al-Zahrani and A. E. Abasaeed, *Catal. Comm.*, 2011, **14**, 107-110.
10. Y.-M. Liu, W.-L. Feng, L.-C. Wang, Y. Cao, W.-L. Dai, H.-Y. He and K.-N. Fan, *Catal. Lett.*, 2006, **106**, 145-152.
11. L. Shi, D. Wang, W. Song, D. Shao, W. P. Zhang and A. H. Lu, *ChemCatChem*, 2017, **9**, 1788-1793.
12. P. Rohani, S. Banerjee, S. Sharifi-Asl, M. Malekzadeh, R. Shahbazian-Yassar, S. J. Billinge and M. T. Swihart, *Adv. Funct. Mater.*, 2019, **29**, 1807788.
13. S. Marchesini, A. Regoutz, D. Payne and C. Petit, *Microporous Mesoporous Mater.*, 2017, **243**, 154-163.
14. M.-Y. Kim, E. A. Kyriakidou, J.-S. Choi, T. J. Toops, A. J. Binder, C. Thomas, J. E. Parks, V. Schwartz, J. Chen and D. K. Hensley, 2016, **187**, 181-194.
15. E. A. Kyriakidou, J. Lee, J.-S. Choi, M. Lance and T. J. Toops, *Catal. Today*, 2020, DOI: https://doi.org/10.1016/j.cattod.2020.1005.1019.
16. J. Chen, B. D. Carlson, T. J. Toops, Z. Li, M. J. Lance, S. G. Karakalos, J.-S. Choi and E. A. Kyriakidou, *ChemCatChem*, 2020, DOI: 10.1002/cctc.202000947.